Chapter 4

Effect of Chemical Forces on Physical Properties

Now how curiously our ideas expand by watching
these conditions of the attraction of cohesion! —
how many new phenomena it gives us beyond
those of the attraction of gravitation!
See how it gives us great strength.

Michael Faraday, *On the Various Forces of Nature*

4.1 Introduction

The forces of attraction between the various ions or atoms in solids determine many of their properties. Intuitively, it is not difficult to appreciate that a strongly bonded material would have a high melting point and stiffness. In addition, it can be shown, as is done below, that its theoretical strength and surface energy will also increase, with a concomitant decrease in thermal expansion. In this chapter, semiquantitative relationships between these properties and the depth and shape of the energy well, described in Chap. 2, are developed.

In Sec. 4.2, the importance of the bond strength on the melting point of ceramics is elucidated. In Sec. 4.3, how strong bonds result in solids with low coefficients of thermal expansion is discussed. In Sec. 4.4, the relationship between bond strength, stiffness, and theoretical strength is developed. Sec. 4.5 relates bond strength to surface energy.

4.2 Melting Points

Fusion, evaporation, and sublimation result when sufficient thermal energy is supplied to a crystal to overcome the potential energy holding its atoms together. Experience has shown that a pure substance at constant pressure will melt at a fixed temperature, with the absorption of heat. The amount

of heat absorbed is known as the **heat of fusion** ΔH_f, and it is the heat required for the reaction

$$\text{Solid} \rightarrow \text{Liquid}$$

ΔH_f is a measure of the enthalpy difference between the solid and liquid states at the melting point. Similarly, the entropy difference ΔS_f between the liquid and solid is defined by

$$\Delta S_f = \frac{\Delta H_f}{T_m} \tag{4.1}$$

where T_m is the melting point in Kelvin. The entropy difference ΔS_f is a direct measure of the degree of disorder that arises in the system during the melting process and is by necessity positive, since the liquid state is always more disordered than the solid. The melting points and ΔS_f values for a number of ceramics are listed in Table 4.1, which reveals that in general as a class, ceramics have higher melting temperatures than, say, metals or polymers. Inspection of Table 4.1 also reveals that there is quite a bit of variability in the melting points.[35] To understand this variability, one needs to understand the various factors that influence the melting point.

4.2.1 Factors Affecting Melting Points of Ceramics that are Predominantly Ionically Bonded

Ionic charge

The most important factor determining the melting point of a ceramic is the bond strength holding the ions in place. In Eq. (2.15), the strength of an ionic bond E_{bond} was found to be proportional to the product of the ionic charges z_1 and z_2 making up the solid. It follows that the greater the ionic charges, the stronger the attraction between ions, and consequently the higher the melting point. For example, both MgO and NaCl crystallize in the rock salt structure, but their melting points are, respectively, 2852 and 800°C — a difference directly attributable to the fact that MgO is made up of doubly ionized ions, whereas in NaCl the ions are singly ionized. Said otherwise, everything else being equal, the energy well of MgO is roughly 4 times deeper than that of NaCl. It is therefore not surprising that it requires more thermal energy to melt MgO than it does to melt NaCl.

[35] Interestingly enough, for most solids including metals, the entropy of fusion per ion lies in the narrow range between 10 and 12 J/(mol · deg). This is quite remarkable, given the large variations in the melting points observed, and strongly suggests that the structural changes on the atomic scale due to melting are similar for most substances. This observation is even more remarkable when the data for the noble-gas solids such as Ar are included — for Ar with a melting point of 83 K, $\Delta S_f = 14$ J/mol · K.

Table 4.1 Melting points and entropies of fusion for selected inorganic compounds

Compound	Melting point, °C	Entropy of fusion, J/mol · °C	Compound	Melting point, °C	Entropy of fusion, J mol · °C
		Oxides			
Al_2O_3	2054 ± 6	47.70	Mullite	1850	
BaO	2013	25.80	Na_2O (α)	1132	33.90
BeO	2780 ± 100	30.54	Nb_2O_5	1512 ± 30	58.40
Bi_2O_3	825		Sc_2O_3	2375 ± 25	
CaO	2927 ± 50	24.80	SrO	2665 ± 20	25.60
Cr_2O_3	2330 ± 15	49.80	Ta_2O_5	1875 ± 25	
Eu_2O_3	2175 ± 25		ThO_2	3275 ± 25	
Fe_2O_3	Decomposes at 1735 K to Fe_3O_4 and oxygen		TiO_2 (rutile)	1857 ± 20	31.50
			UO_2	2825 ± 25	
Fe_3O_4	1597 ± 2	73.80	V_2O_5	2067 ± 20	
Li_2O	1570	32.00	Y_2O_3	2403	≈38.70
Li_2ZrO_3	1610		ZnO	1975 ± 25	
Ln_2O_3	2325 ± 25		ZrO_2	2677	29.50
MgO	2852	25.80			
		Halides			
AgBr	434		LiBr	550	
AgCl	455		LiCl	610	22.60
CaF_2	1423		LiF	848	
CsCl	645	22.17	LiI	449	
KBr	730		NaCl	800	25.90
KCl	776	25.20	NaF	997	
KF	880		RbCl	722	23.85
		Silicates and other glass-forming oxides			
B_2O_3	450 ± 2	33.20	$Na_2Si_2O_5$	874	31.00
$CaSiO_3$	1544	31.00	Na_2SiO_3	1088	38.50
GeO_2	1116		P_2O_5	569	
$MgSiO_3$	1577	40.70	SiO_2 (high quartz)	1423 ± 50	4.60
Mg_2SiO_4	1898	32.76			
		Carbides, nitrides, borides, and silicides			
B_4C	2470 ± 20	38.00	ThN	2820	
HfB_2	2900		TiB_2	2897	
HfC	3900		TiC	3070	
HfN	3390		TiN	2947	
HfSi	2100		$TiSi_2$	1540	
$MoSi_2$	2030		UC	2525	
NbC	3615		UN	2830	
NbN	2204		VB_2	2450	
SiC	2837		VC	2650	
Si_3N_4	At 2151 K partial pressure of N_2 over Si_3N_4 reaches 1 atm		VN	2177	
			WC	2775	
			ZrB_2	3038	
TaB_2	3150		ZrC	3420	
TaC	3985		ZrN	2980 ± 50	
$TaSi_2$	2400		$ZrSi_2$	1700	
ThC	2625				

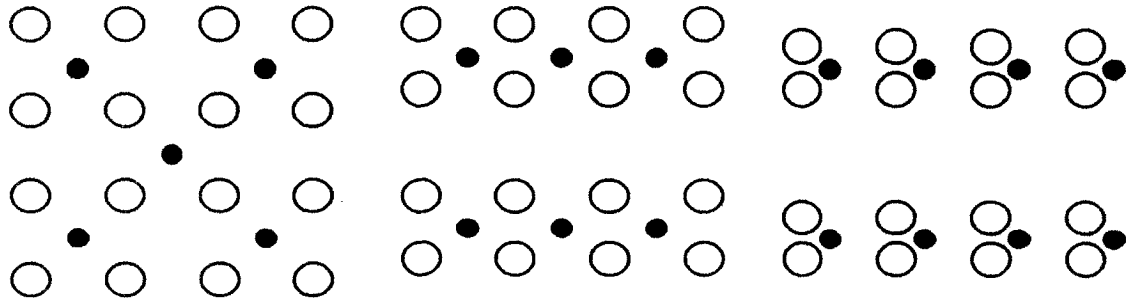

Figure 4.1 Effect of polarization on crystal structure and melting temperature.

Covalent character of the ionic bond

Based on Eq. (4.1), melting points are proportional to ΔH_f, and consequently whatever reduces one reduces the other. It turns out, as discussed below, that increasing the covalent character of a bond tends to reduce ΔH_f by stabilizing discrete units in the melt, which in turn reduces the number of bonds that have to be broken during melting, which is ultimately reflected in lower melting points.

It is important to note that covalency per se does not necessarily favor either higher or lower melting points. The important consideration depends on the melt structure; if the strong covalent bonds have to be broken in order for melting to occur, extremely high melting temperatures can result. Conversely, if the strong bonds do not have to be broken for melting, the situation can be quite different.[36]

The effect of covalency on the structures of three MX_2 compounds is shown graphically in Fig. 4.1. In the figure, the covalent character of the bond increases in going from left to right, which results in changes in the structure from three-dimensional in TiO_2, to a layered structure for CdI_2, to a molecular lattice in the case of CO_2. Also shown in Fig. 4.1 are the corresponding melting points; the effect of the structural changes on the latter is obvious.

It follows from this brief introduction that in order to understand the subtleties in melting point trends, one needs to somewhat quantify the extent of covalency present in an ionic bond. In Chap. 2, the bonds between ions were assumed to be either predominantly covalent or ionic. As noted then, and reiterated here, the reality of the situation is more complex — ionic bonds possess covalent character and vice versa. Historically, this complication has been addressed by means of one of two approaches. The

[36] An extreme example of this phenomenon occurs in polymers, where the bonding is quite strong within the chains and yet the melting points are quite low, because these bonds do not have to be broken during melting.

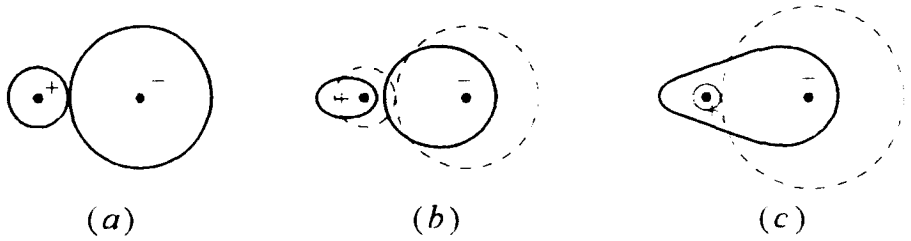

Figure 4.2 Polarization effects: (*a*) idealized ion pair with no polarization; (*b*) polarized ion pair; (*c*) polarization sufficient to form covalent bond.

first was to assume that the bond is purely covalent and then consider the effect of shifting the electron cloud toward the more electronegative atom. The second approach, discussed below, was to assume the bond is purely ionic and then impart a covalent character to it.

The latter approach was championed by Fajans[37] and is embodied in Fajans' rules, whose basic premise is summarized in Fig. 4.2. In Fig. 4.2*a* an idealized ion pair is shown for which the covalent character is nonexistent (i.e., the ions are assumed to be hard spheres). In Fig. 4.2*b* some covalent character is imparted by shifting the electron cloud of the more polarizable anion toward the polarizing cation. In the extreme case that the cation is totally embedded in the electron cloud of the anion (Fig. 4.2*c*) a strong covalent bond is formed. The extent to which the electron cloud is distorted and shared between the two ions is thus a measure of the covalent character of that bond. The covalent character thus defined depends on three factors:

Polarizing power of cation. High charge and small size increase the polarizing power of cations. Over the years many functions have been proposed to quantify the effect, and one of the simplest is to define the **ionic potential** of a cation as:

$$\phi = \frac{z^+}{r}$$

where z^+ is the charge on the cation and r its radius. The ionic powers of a few selected cations are listed in Table 4.2, where it is clear that high charge and small size greatly enhance ϕ and consequently the covalent character of the bond.

To illustrate compare MgO and Al_2O_3. On the basis of ionic charge alone, one would expect the melting point of Al_2O_3 (+3, −2) to be higher than that of MgO (−2, +2), and yet the reverse is observed. However, based on the relative polarizing power of Al^{3+} and Mg^{2+}, it is reasonable to conclude that the covalent character of the Al–O bond is greater than

[37] K. Fajans, *Struct. Bonding*, **2**:88 (1967).

Table 4.2 Ionic potential of selected cations, 1/nm

Li^+	17.0	Be^{2+}	64.0	B^{3+}	150.0
Na^+	10.5	Mg^{2+}	31.0	Al^{3+}	60.0
K^+	7.0	Ca^{2+}	20.0	Si^{4+}	100.0

that of the Mg–O bond. This greater covalency appears to stabilize discrete units in the liquid state and lower the melting point. Further evidence that the Al_2O_3 melt is more "structured" than MgO is reflected in the fact that ΔS_{fusion} *per ion* for Al_2O_3 [9.54 J/(mol · K)] is smaller than that of MgO [12.9 J/(mol · K)].

Polarizability of anions. The *polarizability* of an ion is a measure of the ease with which its electron cloud can be pulled away from the nucleus, which, as discussed in greater detail in Chap. 14, scales with the cube of the radius of the ion, i.e., its volume. Increasing polarizability of the anion increases the covalent character of the bond, which once again results in lower melting points. For example, the melting points of LiCl, LiBr, and LiI are, respectively, 613, 547, and 446°C.[38]

Electron configuration of cation. The *d* electrons are less effective in shielding the nuclear charge than the *s* or *p* electrons and are thus more polarizing. Thus ions with *d* electrons tend to form more covalent bonds. For example, Ca^{2+} and Hg^{2+} have very similar radii (114 and 116 pm, respectively); and yet the salts of Hg have lower melting points than those of Ca — $HgCl_2$ melts at 276°C, whereas $CaCl_2$ melts at 782°C.

4.2.2 Covalent Ceramics

The discussion so far has focused on understanding the relationship between the interatomic forces holding atoms together and the melting points of mostly ionic ceramics. The melting points and general thermal stability of covalent ceramics are quite high as a result of the very strong primary bonds that form between Si and C, N, or O. Covalent ceramics are very interesting materials in that some do not melt but rather decompose at higher temperatures. For example, Si_3N_4 decomposes at temperatures in excess of 2000°C, with the partial pressure of nitrogen reaching 1 atm at those temperatures.

[38] Another contributing factor to the lowering of the melting point that cannot be ignored is the fact that increasing the radii of the anions decreases E_{bond} by increasing r_0. This is a second-order effect, however.

4.2.3 Glass Forming Liquids

These include SiO_2, many of the silicates, B_2O_3, GeO_2, and P_2O_5. What is remarkable about these oxides is that they possess anomalously low entropies of fusion. For SiO_2, ΔS_f is 4.6 J/(mol·K). This signifies that at the melting point, the solid and liquid structures are quite similar. Given that glasses can be considered supercooled liquids, it is not surprising that these oxides, called *network formers*, are the basis of many inorganic glasses (see Chap. 9 for more details).

4.3 Thermal Expansion

It is well known that solids expand upon heating. The extent of the expansion is characterized by a **coefficient of linear expansion** α, defined as the fractional change in length with change in temperature at constant pressure, or

$$\alpha = \frac{1}{l_0}\left(\frac{\partial l}{\partial T}\right)_p \tag{4.2}$$

where l_0 is the original length.

The origin of thermal expansion can be traced to the anharmonicity or asymmetry of the energy distance curve described in Chap. 2 and reproduced in Fig. 4.3. The asymmetry of the curve expresses the fact that it is easier to pull two atoms apart than to push them together. At 0 K, the total energy of the atoms is potential, and the atoms are sitting at the bottom of the well

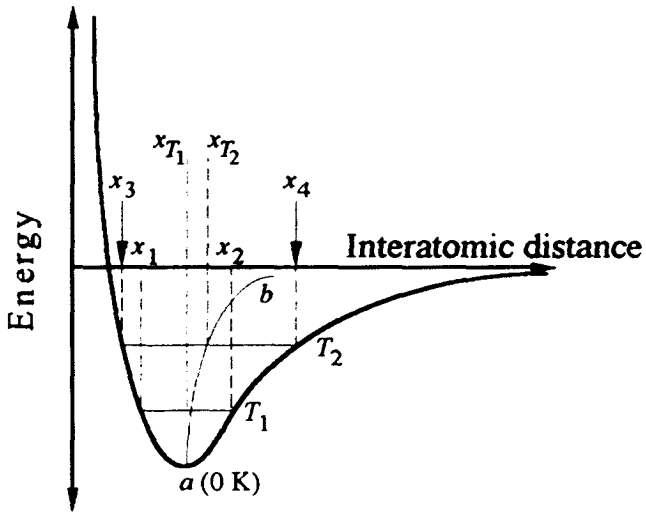

Figure 4.3 Effect of heat on interatomic distance between atoms. Note that asymmetry of well is responsible for thermal expansion. The average position of the atoms in a perfectly symmetric well would not change with temperature.

(point *a*). As the temperature is raised to, say T_1, the average energy of the system increases correspondingly. The atoms vibrate between positions x_1 and x_2, and their energy fluctuates between purely potential at x_1 and x_2 (i.e., zero kinetic energy) and speed up somewhere in between. In other words, the atoms behave if they were attached to each other by springs. The average location of the atoms at T_1 will thus be midway between x_1 and x_2, that is, at x_{T_1}. If the temperature is raised to, say, T_2, the average position of the atoms will move to x_{T_2}, etc. It follows that with increasing temperature, the average position of the atoms will move along line *ab*, shown in Fig. 4.3, and consequently the dimensions of a crystal will also increase.

In general, the asymmetry of the energy well increases with decreasing bond strength, and consequently the thermal expansion of a solid scales inversely with its bond strength or melting point. For example, the thermal expansion coefficient of solid Ar is on the order of $10^{-3}{}^{\circ}C^{-1}$, whereas for most metals and ceramics (see below) it is closer to $10^{-5}{}^{\circ}C^{-1}$.

Perusal of Table 4.3, in which the *mean* thermal expansion coefficients of a number of ceramics are listed, makes it clear that α for most ceramics lies between 3 and $10 \times 10^{-6}\,{}^{\circ}C^{-1}$. The functional dependence of the fractional increase in length on temperature for a number of ceramics and metals is shown in Fig. 4.4. Given that the slope of these lines is α, one can make the following generalizations:

1. Ceramics in general have lower α values than metals.
2. The coefficient α increases with increasing temperature. This reflects the fact that the energy well becomes more asymmetric as one moves up the well, i.e., with increasing temperature. Thus it is important to specify the temperature range reported, since as the temperature range is expanded, the mean thermal expansion coefficient will also increase.
3. Covalently bonded ceramics, such as SiC and Si_3N_4, have lower α's than more close-packed ceramic structures such as NaCl and MgO. This is a reflection of the influence of atomic packing on α. In contradistinction to close-packed structures, where all vibrations result in an increase in the dimensions of the crystal, the more open structures of covalent ceramics allow for other modes of vibration that do not necessarily contribute to thermal expansion. In other words, the added thermal energy can result in a change in the bond angles without significant change in bond length. (Think of the atoms as vibrating into the "open spaces" rather than against each other.)

   One of most striking examples of the importance of atomic packing on α is silica. Vitreous silica has an extremely low α, whereas quartz and cristobalite have much higher thermal expansion coefficients, as shown in Fig. 4.5.

Table 4.3 Mean thermal expansion coefficients and theoretical densities of various ceramics

Ceramic	Theo. density, g/cm^3	$\alpha(^\circ C^{-1}) \times 10^6$	Ceramic	Theo. density, g/cm^3	$\alpha(^\circ C^{-1}) \times 10^6$
		Binary Oxides			
α-Al_2O_3	3.98	7.2–8.8	Nb_2O_5	4.47	
BaO	5.72	17.8	SiO_2(low cristabolite)	2.32	
BeO	3.01	8.5–9.0 (25–1000)	SiO_2(low quartz)	2.65	
Bi_2O_3 (α)	8.90	14.0 (RT–730°C)	ThO_2	9.86	9.2
Bi_2O_3 (δ)	8.90	24.0 (650–825°C)	TiO_2	4.25	8.5
			UO_2	10.96	10.0
CeO_2	7.20		WO_2	7.16	
Cr_2O_3	5.22		Y_2O_3	5.03	9.3 (25–1000)
Dy_2O_3	7.80	8.5			
Gd_2O_3	7.41	10.5	ZnO	5.61	8.0 (c axis)
Fe_3O_4	5.24				4.0 (a axis)
Fe_2O_3	5.18		ZrO_2 (monoclinic)	5.83	7.0
HfO_2	9.70	9.4–12.5			
MgO	3.60	13.5	ZrO_2 (tetragonal)	6.10	12.0
Na_2O	2.27				
		Mixed oxides			
$Al_2O_3 \cdot TiO_2$		9.7 (average)	Cordierite	2.51	2.1
$Al_2O_3 \cdot MgO$	3.58	7.6	$MgO \cdot SiO_2$		10.8 (25–1000)
$5Al_2O_3 \cdot 3Y_2O_3$		8.0 (25–1400)	$2MgO \cdot SiO_2$		11.0 (25–1000)
$BaO \cdot TiO_2$	5.80				
$BaO \cdot ZrO_2$		8.5 (25–1000)	$MgO \cdot TiO_2$		7.9 (25–1000)
$BeO \cdot Al_2O_3$	3.69	6.2–6.7	$MgO \cdot ZrO_2$		12.0 (25–1000)
$CaO \cdot HfO_2$		3.3 (25–1000)	$2SiO_2 \cdot 3Al_2O_3$ (mullite)	3.20	5.1 (25–1000)
$CaO \cdot SiO_2$(β)		5.9 (25–700)	$SiO_2 \cdot ZrO_2$ (zircon)	4.20	4.5 (25–1000)
$CaO \cdot SiO_2$ (α)		11.2 (25–700)	$SrO \cdot TiO_2$		9.4 (25–1000)
$CaO \cdot TiO_2$		14.1			
$CaO \cdot ZrO_2$		10.5	$SrO \cdot ZrO_2$		9.6
$2CaO \cdot SiO_2$ (β)		14.4 (25–1000)	$TiO_2 \cdot ZrO_2$		7.9 (25–1000)

Table 4.3 *Continued*

Ceramic	Theo. density, g/cm^3	$\alpha(^\circ C^{-1}) \times 10^6$	Ceramic	Theo. density, g/cm^3	$\alpha(^\circ C^{-1}) \times 10^6$
		Borides, nitrides; carbides; and silicides			
AlN	3.26	5.6 (25–1000)	TaC	14.48	6.3
			TiB_2	4.50	7.8
B_4C	2.52	5.5	TiC	4.95	7.7–9.5
BN	2.27	4.4	TiN	5.40	9.4
Cr_3C_2	6.68	10.3	$TiSi_2$	4.40	10.5
$CrSi_2$	4.40		Ti_3SiC_2	4.51	9.1
HfB_2	11.20	5.0	WC	15.70	
HfC	12.60	6.6	ZrB_2	6.11	5.7–7.0
$HfSi_2$	7.98		ZrC	6.70	6.9 (25–1000)
$MoSi_2$	6.24	8.5			
β-Mo_2C	9.20	7.8	$ZrSi_2$	4.90	7.6 (25–2700)
NbC	7.78	6.6			
Si_3N_4	3.20	3.1–3.7	ZrN	7.32	7.2
SiC	3.20	4.3–4.8			
		Halides			
CaF_2	3.20	24.0	LiCl	2.07	12.2
LiF	2.63	9.2	LiI	4.08	16.7
LiBr	3.46	14.0	MgF_2		16.0
KI	3.13		NaCl	2.16	11.0
		Glasses			
Soda-lime glass		9.0	Fused silica	2.20	0.55
Pyrex		3.2			

4. Although not explicitly stated, the discussion so far is only strictly true for isotropic, e.g., cubic, polycrystalline materials. Crystals that are noncubic and consequently are anisotropic in their thermal expansion coefficients behave quite differently. In some cases, a crystal can actually shrink in one direction as it expands in another. When a polycrystal is made up of such crystals, the average thermal expansion can be very small, indeed. Cordierite and lithium-aluminosilicate (LAS) (see Fig. 4.4) are good examples of this class of materials. As discussed in greater detail in Chap. 13, this anisotropy in thermal expansion, which has been exploited to fabricate very low-α materials, can result in the buildup of large thermal residual stresses that can be quite detrimental to the strength and integrity of ceramic parts.

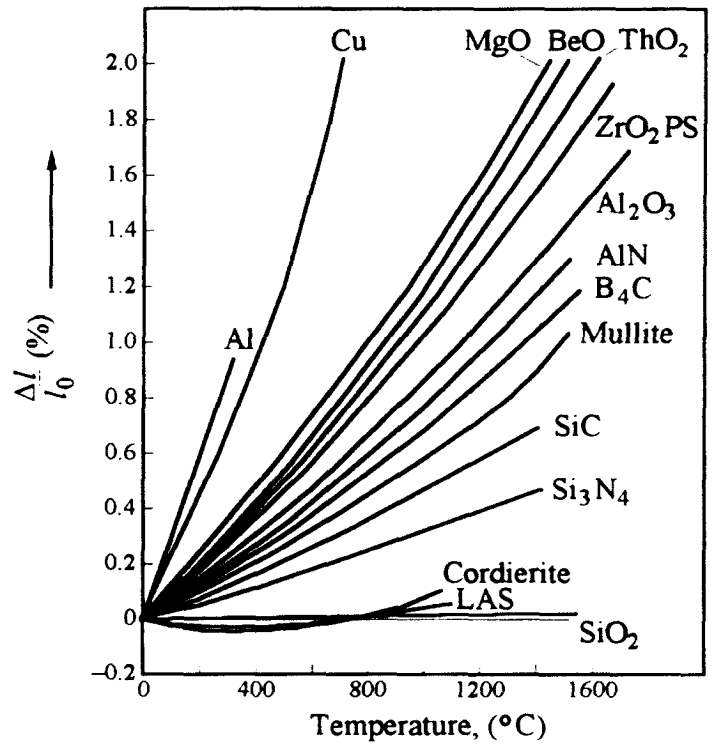

Figure 4.4 $\Delta L/L_0$ (%) versus temperature for a number of ceramics. The slopes of these lines at any temperature are α. For most ceramics, α is more or less constant with temperature. For anisotropic solids, the c axis expansion is reported.[39]

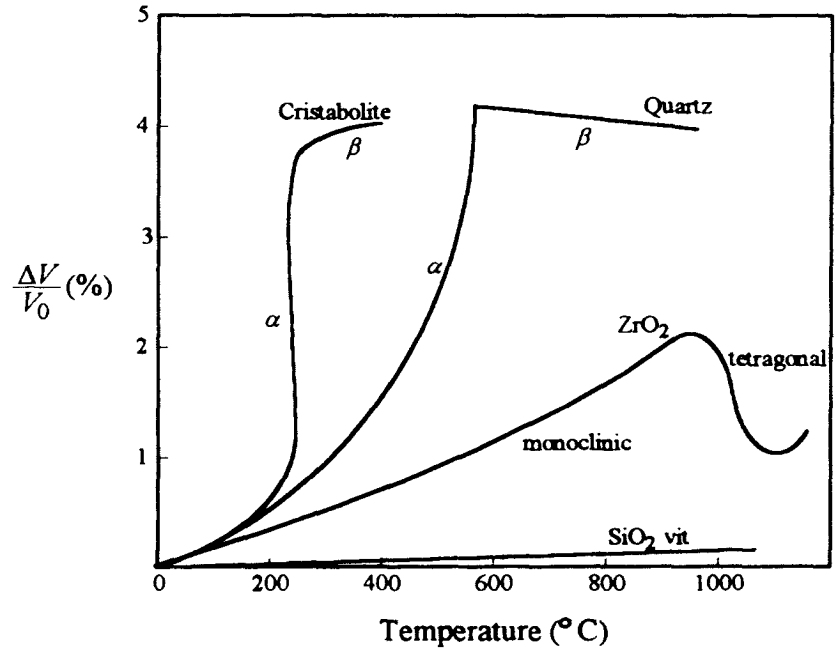

Figure 4.5 $\Delta V/V_0$ (%) versus temperature for cristobalite, quartz, zirconia, and vitreous or amorphous SiO_2.[40] The abrupt changes in behavior with temperature are a result of phase transformations (see Chap. 8).

[39] Adapted J. Chermant, *Les Ceramiques Thermomechaniques*, CNRS Presse, France, 1989.

[40] Adapted from W. D. Kingery, H. K. Bowen, and D. R. Uhlmann, *Introduction to Ceramics*, 2d ed., Wiley, New York, 1976.

4.4 Young's Modulus and the Strength of Perfect Solids

In addition to understanding the behavior of ceramics exposed to thermal energy, it is important to understand their behavior when they are subjected to an external load or stress. The objective of this section is to interrelate the shape of the energy versus distance curve $E(r)$, discussed in Chap. 2, to the elastic modulus, which is a measure of the stiffness of a material and the theoretical strength of that material. To accomplish this goal, one needs to examine the forces $F(r)$ that develop between atoms as a result of externally applied stresses. As noted in Sec. 2.4, $F(r)$ is defined as

$$F(r) = \frac{dE(r)}{dr} \tag{4.3}$$

From the general shape of the $E(r)$ curve, one can easily sketch the shape of a typical force versus distance curve, as shown in Fig. 4.6. The following salient features are noteworthy:

- The net force between the atoms or ions is zero at equilibrium, i.e., at $r = r_0$.
- Pulling the atoms apart results in the development of an *attractive restoring force* between them that tends to pull them back together. The opposite is true if one tries to push the atoms together.
- In the region around $r = r_0$ the response can be considered, to a very good approximation, linear (inset in Fig. 4.6). In other words, the atoms act as if

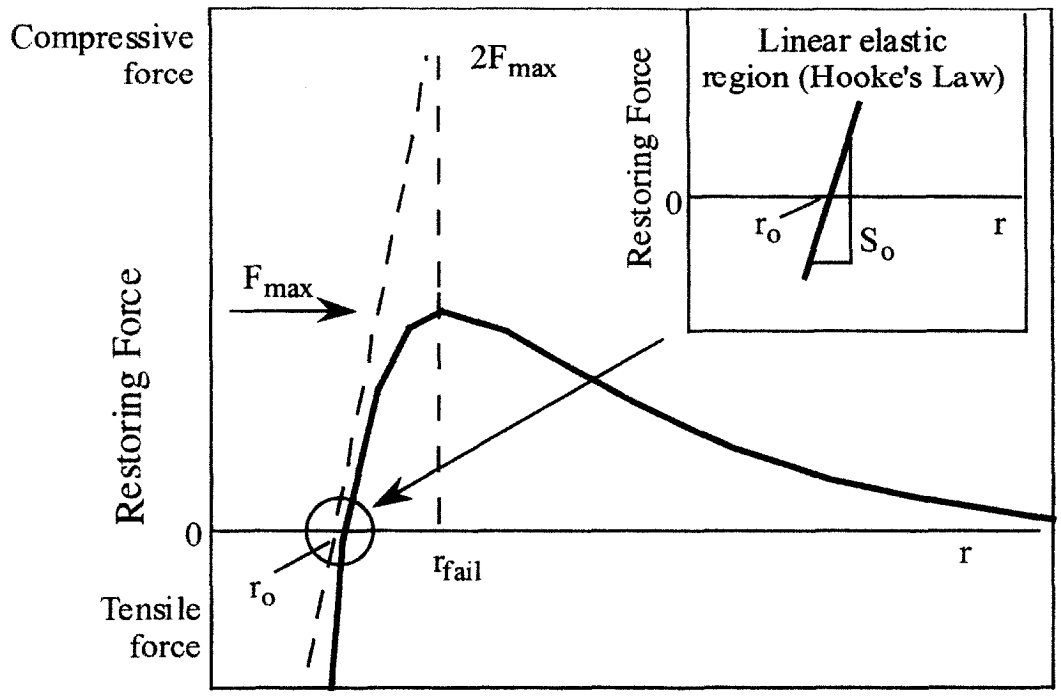

Figure 4.6 Typical force–distance curve. Slope of line going through r_0 is the stiffness of the bond S_0. It is assumed in this construction that the maximum force is related to the stiffness as shown. This is quite approximate but serves to illustrate the relationship between stiffness and theoretical strength i.e. Eq. (4.12).

they are tied together by miniature springs. It is in this region that Hooke's law (see below) applies.

- The force pulling the atoms apart cannot be increased indefinitely. Beyond some separation r_{fail}, the bond will fail. The force at which this occurs represents the maximum force F_{max} that the bond can withstand before failing.

In the remainder of this section, the relationships between stiffness and theoretical strength, on one hand, and $E(r)$ and $F(r)$, on the other hand, are developed.

An atomic view of Young's modulus

Experience has shown that all solids will respond to small stresses σ by stretching in proportion to the stress applied, a phenomenon that is described by **Hooke's law**:

$$\sigma = Y\varepsilon \tag{4.4}$$

where Y is Young's modulus and ε is the **strain** experienced by the material, defined as

$$\varepsilon = \frac{L - L_0}{L_0} \tag{4.5}$$

Here L is the length under the applied stress, and L_0 is the original length.

Refer once more to the force/distance curve shown in Fig. 4.6. In the vicinity of r_0, the following approximation can be made:

$$F = S_0(r - r_0) \tag{4.6}$$

where S_0 is the **stiffness** of the bond, defined as

$$S_0 = \left(\frac{dF}{dr}\right)_{r=r_0} \tag{4.7}$$

Note that Eq. (4.6) is nothing but an expression for the extension of a linear spring.

Dividing Eq. (4.6) by r_0^2 and noting that F/r_0^2 is approximately the stress on the bond, while $(r - r_0)/r_0$ is the strain on the bond, and comparing the resulting expression with Eq. (4.4), one can see immediately that

$$\boxed{Y \approx \frac{S_0}{r_0}} \tag{4.8}$$

Combining this result with Eqs. (4.3) and (4.7), it is easy to show that

$$Y = \frac{1}{r_0}\left(\frac{dF}{dr}\right)_{r=r_0} = \frac{1}{r_0}\left(\frac{d^2E}{dr^2}\right)_{r=r_0} \tag{4.9}$$

This is an important result because it says that the stiffness of a solid is directly related to the curvature of its energy/distance curve. Furthermore, it implies that strong bonds will be stiffer than weak bonds; a result that is not in the least surprising, and it explains why, in general, given their high melting temperatures, ceramics are quite stiff solids.

Theoretical strengths of solids

The next task is to estimate the theoretical strength of a solid or the stress that would be required to *simultaneously* break all the bonds across a fracture plane. It can be shown (see Prob. 4.2) that typically most bonds will fail when they are stretched by about 25%, i.e., when $r_{\text{fail}} \approx 1.25r_0$. It follows from the geometric construction shown in Fig. 4.6 that

$$S_0 \approx \frac{2F_{\max}}{r_{\text{fail}} - r_0} \approx \frac{2F_{\max}}{1.25r_0 - r_0} \tag{4.10}$$

Dividing both sides of this equation by r_0 and noting that

$$\frac{F_{\max}}{r_0^2} \approx \sigma_{\max} \tag{4.11}$$

i.e., the force divided by the area over which it operates, one obtains

$$\sigma_{\max} \approx \frac{Y}{8} \tag{4.12}$$

For a more exact calculation, one starts with the energy/interatomic distance function in its most general form, i.e.,

$$E_{\text{bond}} = \frac{C}{r^n} - \frac{D}{r^m} \tag{4.13}$$

where C and D are constants and $n > m$. Assuming $\sigma_{\max} \approx F_{\max}/r_0^2$, one can show (see Prob. 4.2) that $\sigma_{\max}$ is better approximated by

$$\sigma_{\max} = \frac{Y}{[(n+1)/(m+1)]^{(m+1)/(n-m)}} \frac{1}{n+1} \tag{4.14}$$

Substituting typical values for m and n, say, $m = 1$ and $n = 9$, for an ionic bond yields $\sigma_{\max} \approx Y/15$.

Based on these results, one may conclude that the theoretical strength of a solid should be roughly one-tenth of its Young's modulus. Experience has shown, however, that the actual strengths of ceramics are much lower and are closer to $Y/100$ to $Y/1000$. The reason for this state of affairs is discussed in greater detail in Chap. 11, and reflects the fact that real solids are not perfect, as assumed here, but contain many flaws and defects that tend to locally concentrate the applied stress, which in turn significantly weaken the material.

4.5 Surface Energy

The **surface energy** γ of a solid is the amount of energy needed to create a unit area of new surface. The process can be pictured as shown in Fig. 4.7*a*, where two new surfaces are created by cutting a solid in two. Given this simple picture, the surface energy is simply the product of the number of bonds N_s broken per unit area of crystal surface and the energy per bond E_{bond}, or

$$\gamma = N_s E_{\text{bond}} \tag{4.15}$$

For the sake of simplicity, only first-neighbor interactions will be considered here, which implies that E_{bond} is given by Eq. (2.15). Also note that since N_s is a function of crystallography, it follows that γ is also a function of crystallography.

To show how to calculate surface energies by starting with Eq. (4.15), consider cleaving a rock salt crystal along its (100) plane,[41] shown in

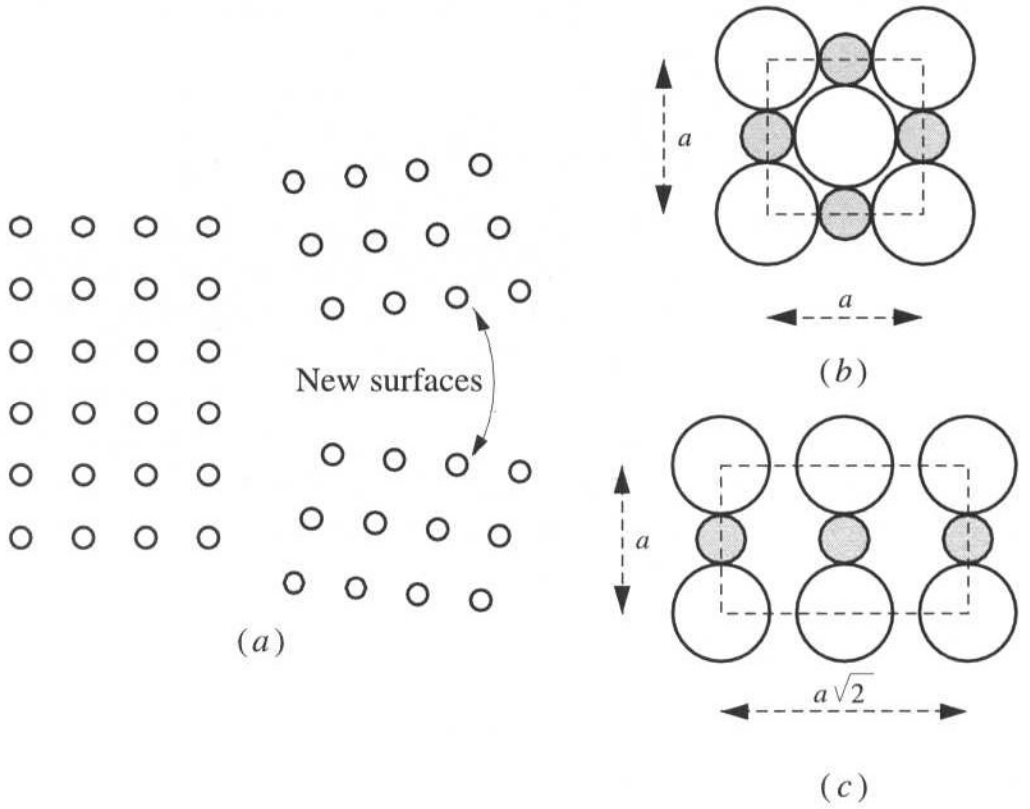

Figure 4.7 (*a*) The creation of new surface entails the breaking of bonds across that surface. (*b*) Structure of (100) plane in the rock salt structure. (*c*) Structure of (110) plane in same structure. Note that the coordination number of ions in this plane is 2, which implies that to create a (110) plane, only two bonds per ion would have to be broken.

[41] It is assumed here that the reader is familiar with Miller indices, a topic that is covered in almost all introductory materials science or engineering textbooks.

Table 4.4 Measured free surface energies of solids

Substance	Surface	Environment	Temp., K	Surface energy, J/m^2
Mica	(0001)	Air	298	0.38
		Vacuum	298	5.00
MgO	(100)	Air	298	1.15
KCl	(100)	Air	298	0.11
Si	(111)	Liquid N_2	77	1.24
NaCl	(100)	Liquid N_2	77	0.32
CaF_2	(111)	Liquid N_2	77	0.45
LiF	(100)	Liquid N_2	77	0.34
$CaCO_3$	$(10\bar{1}0)$	Liquid N_2	77	0.23

Fig. 4.7*b*. This plane contains two cations and two anions and has an area of $(2r_0)^2$, where r_0 is the equilibrium interionic distance. Note, however, that the total surface area created is twice that, or $2 \times (2r_0)^2$. Since four bonds have to be broken, it follows that $N_s = 4/[2 \times (2r_0)^2]$. Combining this result with Eqs. (2.15) and (4.15) yields

$$\gamma_{100} \approx -E_{\text{bond}}\left[\frac{4}{2(2r_0)^2}\right] \approx -\frac{z_1 z_2 e^2}{8\pi\varepsilon_0 r_0^3}\left(1 - \frac{1}{n}\right) \tag{4.16}$$

The minus sign is introduced because energy has to be consumed to create a surface. Calculations of surface energies based on Eq. (4.16) invariably yield values that are substantially greater than the measured ones (see Table 4.4). The reason for this discrepancy comes about because in the simple model, surface relaxation and rearrangement of the atoms upon the formation of the new surface were not allowed. When the surface is allowed to relax, much of the energy needed to form it is recovered, and the theoretical predictions do indeed approach the experimentally measured ones.

WORKED EXAMPLE 4.1

Estimate the surface energy of the (100) and (110) planes in NaCl, and compare your results with those listed in Table 4.4.

Answer

For NaCl, $r_0 = 2.83 \times 10^{-10}$ m, which when substituted in Eq. (4.16), assuming $n = 9$ yields a value for the surface energy of $\approx 4.5\ J/m^2$. By comparing this value with the experimentally measured value listed in Table 4.4, it is immediately obvious that it is off by more than an order of magnitude, for reasons alluded to above.

The (110) plane (Fig. 4.7*c*) has an area of $\sqrt{2}(2r_0)(2r_0)$ but still contains two Na and two Cl ions. However, the coordination number of each of the atoms in the plane is now 2 instead of 4, which implies that each ion is coordinated to *two* other ions above and below the plane (here, once again for simplicity, all but first-neighbor interactions are considered). In other words, to create the plane, one needs to break two bonds per ion. It follows that

$$N_s = \frac{2 \times 4}{2\sqrt{2}(2r_0)^2} \text{ bonds/m}^2$$

and the corresponding surface energy is thus $6.36\,\text{J/m}^2$.
Note that the easiest way to calculate N_s is to appreciate that:

$$N_s = (\text{CN-CN}_\text{p})/2$$

where CN is the coordination number, i.e. number of nearest neighbors of opposite charge in the crystal and CN_p is the coordination number of ions in surface formed. For e.g. in Fig. 4.7*c*, CN = 6 and $\text{CN}_\text{p} = 2$. Thus the number of bonds broken = (6 – 2)/2 = 2 Similarly, for a 111 surface, $N_s = (6 - 0)/2 = 3$, etc.

Experimental Details

Melting points

Several methods can be used to measure the melting point of solids. One of the simplest is probably to use a **differential thermal analyser** (DTA for short). The basic arrangement of a differential thermal analyser is simple and is shown schematically in Fig. 4.8*a*. The sample and an inert reference (usually alumina powder) are placed side by side in a furnace, and identical thermocouples are placed below each. The temperature of the furnace is then slowly ramped, and the difference in temperature $\Delta T = T_{\text{sample}} - T_{\text{ref}}$ is measured

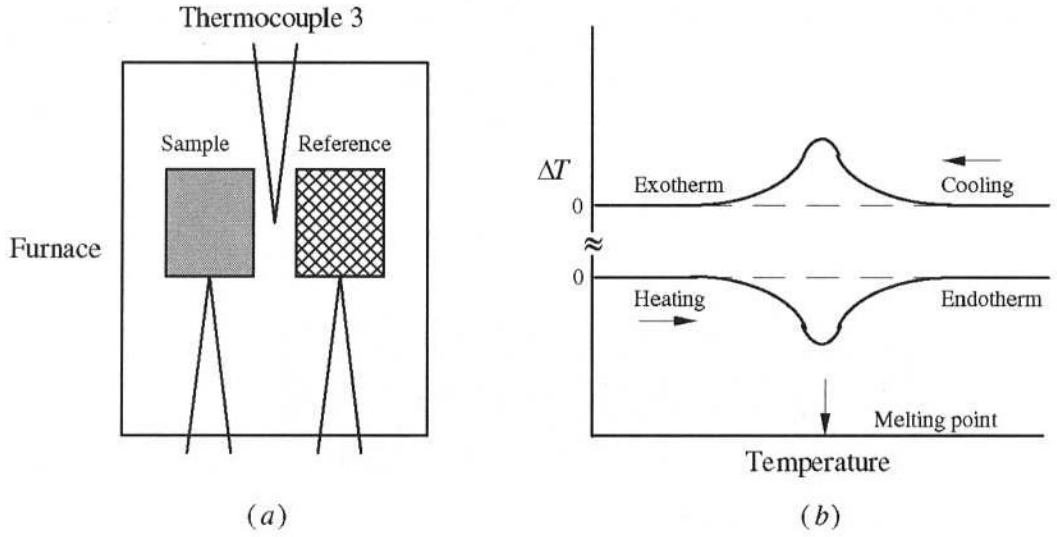

Figure 4.8 (*a*) Schematic of DTA setup. (*b*) Typical DTA traces upon heating (bottom curve) and cooling (top curve).

as a function of the temperature of the furnace, which is measured by a third thermocouple (thermocouple 3 in Fig. 4.8*a*). Typical results are shown in Fig. 4.8*b* and are interpreted as follows. As long as both the sample and the reference are inert, they should have the same temperature and $\Delta T = 0$. However, if for any reason the sample absorbs (endothermic process) or gives off (exothermic process) heat, its temperature vis-à-vis the reference thermocouple will change accordingly. For example, melting, being an endothermic process, will appear as a trough upon heating. The melting point is thus the temperature at which the trough appears. In contrast, upon cooling, freezing, being an exothermic process, will appear as a peak.

Thermal expansion coefficients

Thermal expansion coefficients are measured with a dilatometer, which is essentially a high-temperature furnace from which a rod sticks out (Fig. 4.9). One side of the rod is pushed against the sample for which the thermal expansion is to be measured, and the other side is attached to a device that can measure the displacement of the rod very accurately, such as a linear variable differential transformer or LVDT. In a typical experiment, the sample is placed inside the furnace and is heated at a constant rate, while simultaneously the displacement of the push rod is measured. Typical curves for a number of ceramics and metals are shown in Fig. 4.4.

Surface energies

A variety of methods can be used to measure the surface energy of ceramics. One technique, of limited applicability (see below), is to measure the force needed to cleave a crystal by starting with an atomically sharp notch of length c. In Chap. 11, the following relationship between the surface energy, Young's modulus, and the applied stress at fracture σ_{app} is derived:

$$\gamma = \frac{A' c \sigma_{app}^2}{2Y} \tag{4.17}$$

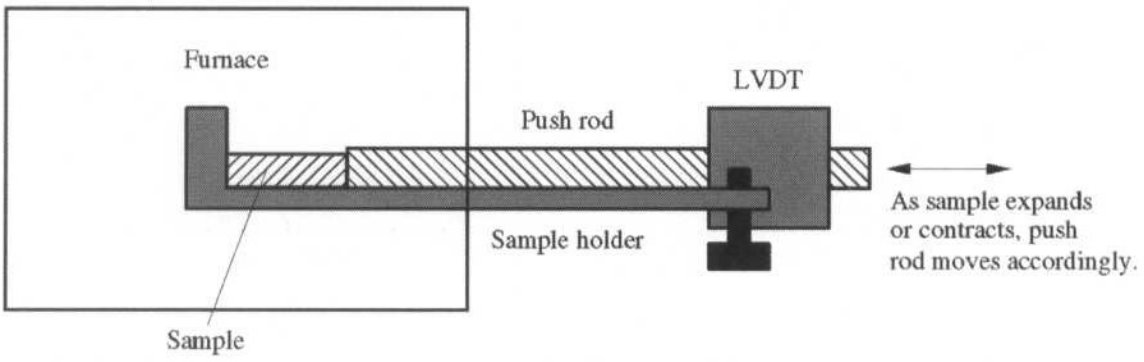

Figure 4.9 Schematic of a dilatometer.

where A' is a geometric factor that depends on the loading conditions and the specimen geometry. Once σ_{app} is measured for a given c, γ is easily calculated from Eq. (4.17) if the modulus is known. In deriving this equation, it is implicit that all the mechanical energy supplied by the testing rig goes into creating the new surfaces. Also implicit is that there were no energy-consuming mechanisms occurring at the crack tip, such as dislocation movements; i.e., the failure was a pure brittle failure. It is important to note that this condition is only satisfied for a small number of ionic and covalent ceramics, some of which are listed in Table 4.4.

4.6 Summary

1. The strengths of the bonds between atoms or ions in a solid, by and large, determine many of its properties, such as its melting and boiling points, stiffness, thermal expansion, and theoretical strength.
2. The stronger the bond, the higher the melting point. However, partial covalency to an ionic bond will tend to stabilize discrete units in the melt and lower the melting point.
3. Thermal expansion originates from the anharmonic vibrations of atoms in a solid. The asymmetry of the energy well is a measure of the thermal expansion coefficient α, with stronger bonds resulting in more symmetric energy wells and consequently lower values of α. In addition, the atomic arrangement can play an important role in determining α.
4. As a first approximation, the curvature of the energy/distance well is a measure of the stiffness or Young's modulus of a solid. In general, the stronger the bond, the stiffer the solid. Other factors such as atomic arrangement are also important, however.
5. The theoretical strength of a bond is on the order of $Y/10$. The actual strengths of ceramics, however, are much lower for reasons to be discussed in Chap. 11.
6. The surface energy of a solid not only scales with the bond energy but also depends on crystallographic orientation.

Problems

4.1. (*a*) The equilibrium interatomic spacings of the Na halides and their melting points are listed below. Explain the trend observed.

	NaF	NaCl	NaBr	NaI
Spacing, nm	0.23	0.28	0.29	0.32
Melting point, °C	988	801	740	660

(*b*) Explain the melting point trends observed for the alkali metal chlorides as one goes from HCl (−115.8°C) to CsCl.

(*c*) Which of these pairs of compounds would you expect to have the higher melting points; CaF_2 versus ZrO_2; UO_2 versus CeO_2; CaF_2 versus CaI_2? Explain.

4.2. Starting with Eq. (4.13) in text, do the following:

(*a*) Derive the following relationship:

$$S_0 = \frac{mD}{r_0^{m+2}}(n - m)$$

Using this equation, calculate S_0 for NaCl. Assume $n = 9$.

Hint: Show that for an ionic bond $D = \dfrac{z_i z_2 e^2}{4\pi\varepsilon_0}$

Answer: 81 N/m

(*b*) Derive the following expression for Young's modulus. State all assumptions.

$$Y \approx \frac{mD}{r_0^{m+3}(n - m)}$$

(*c*) Show that the distance at which the bond will break r_{fail} is given by

$$r_{\text{fail}} = \left(\frac{n+1}{m+1}\right)^{\frac{1}{n-m}}(r_0)$$

For ionic bonds, $m = 1$ and $n \approx 9$; for van der Waals bonds, $m = 6$ and $n = 12$. Calculate the strain at failure for each bond.

(*d*) Derive Eq. (4.14) in the text, and show that for an ionic bond $\sigma_{\text{fail}} \approx Y/15$.

4.3. (*a*) Show that for the rock salt structure $\gamma_{(111)}/\gamma_{(100)} = \sqrt{3}$.

(*b*) Calculate from first principles the surface energies of the (100) and (111) planes of MgO. How do your values compare with those shown in Table 4.4? Discuss all assumptions.

(*c*) It has been observed that NaCl crystals cleave more easily along the (100) planes than along the (110) planes. Show, using calculations, why you think that is the case.

4.4. Calculate the number of broken bonds per square centimeter for Ge (which has a diamond cubic structure identical to the one shown in Fig. 3.1*c* except that all the atoms are identical) for the (100) and (111) surfaces. Which surface do you think has the lower surface energy? Why? The lattice constant of Ge is 0.565 nm, and its density is 5.32 g/cm^3.

Answer: For (100), 1.25×10^{15} bonds/cm^2 for (111), 0.72×10^{15} bonds/cm^2.

4.5. Take the C–C bond energy to be 376 kJ/mol. Calculate the surface energy of the (111) plane in diamond. Repeat for the (100) plane. Which plane do you think would cleave more easily? Information you may find useful: density of diamond is 3.51 g/cm^3 and its lattice parameter is 0.356 nm.

Answer: $\gamma_{(111)} = 9.820\,\text{J/m}^2$

4.6. Would you expect the surface energies of the Noble-gas solids to be greater than, about the same as, or smaller than those of ionic crystals? Explain.

4.7. Estimate the thermal expansion coefficient of alumina from Fig. 4.4. Does your answer depend on the temperature range over which you carry out the calculation? Explain.

4.8. Estimate the order of magnitude of the maximum displacement of Na and Cl ions in NaCl from their equilibrium position at 300 and at 900 K.

4.9. Prove that the linear expansion coefficient α, with very little loss in accuracy, can be assumed to be one-third that of the volume coefficient for thermal expansion α_v. You can assume that $l = l_0(1 + \alpha)$ and $v = v_0(1 + \alpha_v)$ and $v_0 = l_0^3$.

4.10. (*a*) "A solid for which the energy distance curve is perfectly symmetric would have a large thermal expansion coefficient." Do you agree with this statement? Explain.

(*b*) The potential energy $U(x)$ of a pair of atoms that are displaced by x from their equilibrium position can be written as $U(x) = \alpha x^2 - \beta x^3 - \gamma x^4$, where the last two terms represent the anharmonic part of the well. At any given temperature, the probability of displacement occurring relative to that it will not occur is given by the Boltzmann factor $e^{-U/(kT)}$, from which it follows that the average displacement at this temperature is

$$\bar{x} = \frac{\int_{-\infty}^{\infty} x e^{-U/(kT)}}{\int_{-\infty}^{\infty} e^{-U/(kT)}}$$

Show that at small displacements, the average displacement is

$$\bar{x} = \frac{3\beta kT}{4\alpha^2}$$

What does this final result imply about the effect of the strength of the bond on thermal expansion?

Additional Reading

1. L. Van Vlack, *Elements of Materials Science and Engineering*, 5th ed., Addison-Wesley, Reading, Massachusetts, 1985.
2. N. N. Greenwood, *Ionic Crystals, Lattice Defects and Non-Stoichiometry*, Butterworth, London, 1968.
3. L. Azaroff, *Introduction to Solids*, McGraw-Hill, New York, 1960.
4. J. Huheey, *Inorganic Chemistry*, 2d ed., Harper & Row, New York, 1978.
5. L. Solymar and D. Walsh, *Lectures on the Electrical Properties of Materials*, 4th ed., Oxford University Press, New York, 1988.
6. C. Kittel, *Introduction to Solid State Physics*, 6th ed., Wiley, New York, 1986.
7. B. H. Flowers and E. Mendoza, *Properties of Matter*, Wiley, New York, 1970.
8. A. H. Cottrell, *The Mechanical Properties of Matter*, Wiley, New York, 1964.
9. M. F. Ashby and R. H. Jones, *Engineering Materials*, Pergamon Press, New York, 1980.